

Experimental evidence for transverse wobbling bands in ^{136}Nd

B. F. Lv,^{1,2} C. M. Petrache^{2,*}, R. Budaca,³ A. Astier,² K. K. Zheng,^{1,2} P. Greenlees,⁴ H. Badran,⁴ T. Calverley,^{4,5} D. M. Cox,^{4,†} T. Grahn,⁴ J. Hilton,^{4,5} R. Julin,⁴ S. Juutinen,⁴ J. Konki,^{4,‡} J. Pakarinen,⁴ P. Papadakis,^{4,§} J. Partanen,⁴ P. Rakhila,⁴ P. Ruotsalainen,⁴ M. Sandzelius,⁴ J. Saren,⁴ C. Scholey,⁴ J. Sorri,^{4,6} S. Stolze,^{4,||} J. Uusitalo,⁴ B. Cederwall,⁷ A. Ertoprak,⁷ H. Liu,⁷ S. Guo,¹ J. G. Wang,¹ H. J. Ong,¹ X. H. Zhou,¹ Z. Y. Sun,¹ I. Kuti,⁸ J. Timár,⁸ A. Tucholski,⁹ J. Srebrny,⁹ and C. Andreoiu¹⁰

¹Key Laboratory of High Precision Nuclear Spectroscopy and Center for Nuclear Matter Science, Institute of Modern Physics, Chinese Academy of Sciences, Lanzhou 730000, People's Republic of China

²Université Paris-Saclay, CNRS/IN2P3, IJCLab, 91405 Orsay, France

³“Horia Hulubei” National Institute for Physics and Nuclear Engineering, Str. Reactorului 30, RO-077125, POB-MG6 Bucharest-Măgurele, Romania

⁴Department of Physics, University of Jyväskylä, Jyväskylä FIN-40014, Finland

⁵Department of Physics, University of Liverpool, The Oliver Lodge Laboratory, Liverpool L69 7ZE, United Kingdom

⁶Sodankylä Geophysical Observatory, University of Oulu, FIN-99600 Sodankylä, Finland

⁷KTH Department of Physics, S-10691 Stockholm, Sweden

⁸Institute for Nuclear Research (Atomki), Pf. 51, 4001 Debrecen, Hungary

⁹University of Warsaw, Heavy Ion Laboratory, Pasteura 5a, 02-093 Warsaw, Poland

¹⁰Department of Chemistry, Simon Fraser University, Burnaby, British Columbia, Canada V5A 1S6



(Received 3 December 2021; accepted 23 February 2022; published 2 March 2022)

The nature of two high-spin bands in ^{136}Nd built on the two-quasiparticle configuration $\pi h_{11/2}^2$, predicted by the triaxial projected shell model as good candidates of transverse wobbling bands, are investigated experimentally. The mixing ratio of one $\Delta I = 1$ transition connecting the one-phonon and the zero-phonon wobbling bands is established from a high-statistics JuroGam II γ -ray spectroscopy experiment by using the combined angular correlation and linear polarization method. The resulting wobbling excitation energy and ratios of reduced electromagnetic transition probabilities are in good agreement with results of a new particle-rotor model which rigidly couples the total angular momentum of two quasiparticles to a triaxial core in an orthogonal geometry, confirming thus the transverse wobbling nature of the bands.

DOI: [10.1103/PhysRevC.105.034302](https://doi.org/10.1103/PhysRevC.105.034302)

I. INTRODUCTION

The degree of collective motion is an intriguing subject in the $A \approx 130$ mass region. One possibility is the nuclear wobbling motion, which was first predicted in the high-spin region of the even-even systems by Bohr and Mottelson [1] and is considered as a fingerprint of a triaxial nuclear shape. It is a collective excitation of a deformed nucleus with three unequal moments of inertia which rotates about the axis with the largest moment of inertia, whose orientation executes a low-amplitude oscillation. This exotic phenomenon was observed about 20 years ago in the high-spin regime of several odd- A nuclei of the $A \approx 160$ mass region: ^{161}Lu [2], ^{163}Lu [3,4],

^{165}Lu [5], ^{167}Lu [6], and ^{167}Ta [7]. All observed wobbling bands were based on strongly deformed triaxial shapes with a substantial deviation from axial symmetry ($\epsilon_2 \approx 0.4$, $\gamma \approx \pm 20^\circ$), and have been interpreted using particle-rotor calculations by assuming parallel angular momenta of the odd nucleon and the triaxial core [8,9]. The nature of the $\Delta I = 1$ transitions between the excited and yrast wobbling bands in odd-even nuclei is expected to be predominantly electric since the entire nuclear charge is involved in the wobbling oscillation.

Recently, the wobbling motion in odd-even nuclei was revisited by Frauendorf and Dönau [10], and two types of coupling of the angular momenta of the odd nucleon to the triaxial core have been proposed, with parallel and orthogonal geometry, which lead to transverse and longitudinal wobbling, respectively. The excitation energy of the one-phonon wobbling band relative to the zero-phonon band E_{wob} [see formula (4) in Sec. III] decreases (increases) with increasing spin in the transverse (longitudinal) wobbling mode. However, one must make a distinction between the nature (transverse or longitudinal) of alignment and wobbling, which are not necessarily the same, as the nucleus can rotate around an axis perpendicular to the alignment.

* petrache@ijclab.in2p3.fr

[†]Present address: Department of Physics, Lund University, 22100 Lund, Sweden.

[‡]Present address: CERN, CH-1211 Geneva 23, Switzerland.

[§]Present address: STFC Daresbury Laboratory, Daresbury, Warrington, WA4 4AD, United Kingdom.

^{||}Present address: Physics Division, Argonne National Laboratory, Argonne, Illinois 60439, USA.

Both types of wobbling motion have been recently reported in odd-even nuclei: transverse wobbling bands in ^{135}Pr [10–12] and in ^{105}Pd [13], as well as longitudinal wobbling in ^{133}La [14], ^{187}Au [15], ^{183}Au [16], and ^{127}Xe [17]. However, contrary to the wobbling bands in the $A \approx 160$ mass region, all the recently reported bands develop at low spin, and therefore do not fulfill the high-spin approximation employed by Bohr and Mottelson when deriving the properties of the wobbling bands [1]. In fact, the existence of the low-spin transverse wobbling in nuclei is under current debate, see, e.g., Refs. [18–20]: it was pointed out that the frozen approximation proposed in Ref. [10] appears unrealistic, since it leaves out the effect of the Coriolis force on the quasiparticle which has the angular momentum coupled transversely to that of the core. A new concept of tilted precession (TiP) motion was proposed in the framework of the quasiparticle-triaxial-rotor (QTR) model for triaxial nuclei by Lawrie *et al.* [18]: the three-dimensional rotation can be represented as a precession of the total angular momentum around a certain axis and at a given tilt. It was proven that the zero- and one-quasiparticle bands can be approximated with wobbling motion only at high spin. Currently, based on new experimental data and new theoretical calculations, the recently reported low-spin wobbling bands are seriously questioned [18–28].

Compared with the wobbling motion in odd- A nuclei, the evidence of the wobbling mode in even-even systems is extremely scarce, even though it has been proposed about half a century ago. Experimentally, the only simple wobbler candidates are low-spin bands in the even-even nuclei ^{112}Ru [29] and ^{104}Pd [30] reported around a decade ago. However, the wobbling interpretation of these bands is not fully supported experimentally, the crucial observables for the assignment of the wobbling nature—mixing ratios and transition probabilities of the connecting transitions—being not measured. In addition, these nuclei are expected to have a soft shape. In such cases the γ vibrations are not easy to disentangle from wobbling motion. At medium spin, after the breaking of a nucleon pair, the nucleus acquires a more stable triaxial shape under the effect of rotation and of the polarization induced by the unpaired particles. Thereafter, the existence of one-phonon and possible two-phonon transverse wobbling bands at medium spin (above $I = 10$) was proposed for the first time in two even-even nuclei, ^{134}Ce and ^{136}Nd [31]. However, this conjecture was also not well supported experimentally, due to the lack of measured mixing ratios and transition probabilities of the connecting $\Delta I = 1$ transitions between the proposed wobbling bands. Very recently, the first case of transverse wobbling bands built on the two-quasiparticle $\pi h_{11/2}^2$ configuration in the even-even nucleus ^{130}Ba was reported [32]. The experimental wobbling excitation energy E_{wob} , and the electromagnetic transition probability ratios were in excellent agreement with the constrained triaxial covariant density-functional theory combined with quantum particle rotor model calculations. It is important to note that, at difference from the one-quasiparticle wobbling bands for which the connecting $\Delta I = 1$ transitions between the bands have predominant electric character, in the case of two-quasiparticle wobbling bands the connect-

ing transitions can be predominantly magnetic, because the total gyromagnetic factor of two nucleons can lead to significantly larger magnetic component. The detailed analysis of the bands properties, that is the probability density distributions of the orientation of the angular momenta with respect to the body-fixed frame, and the angular-momentum geometry, demonstrated the transverse geometry of the angular momenta of the unpaired nucleon and the triaxial core. Thus, it supported the presence of transverse wobbling motion in two-quasiparticle bands developing at medium spin in even-even nuclei [32].

The object of the present study is a pair of medium-spin bands of ^{136}Nd , a nucleus which has been intensively investigated previously both experimentally and theoretically. The band structure of ^{136}Nd is very rich, exhibiting multiple chiral bands, octupole bands, highly deformed bands, as well as oblate bands, see Refs. [33–44]. Of particular interest here are the even- and odd-spin two-quasiparticle bands with the $\pi h_{11/2}^2$ configuration which have been recently investigated in detail with the triaxial projected shell model, proposing their interpretation in terms of transverse wobbling motion [44]. Following that paper, the ^{136}Nd nucleus became the second candidate for two-quasiparticle transverse wobbling bands in even-even nuclei. The proposed two-quasiparticle wobbling bands in ^{136}Nd are similar, to a certain extent, to the corresponding bands in ^{130}Ba close to the bandhead, but their evolution with increasing spin is different, the wobbling character being eroded faster in ^{136}Nd . In this work we focus on the measurement of the crucial experimental evidence for the predicted transverse wobbling bands in ^{136}Nd , exploring experimentally the nature of connecting transitions between these bands and comparing the obtained results with the predictions of a newly developed particle-rotor approach [45].

II. EXPERIMENTAL DETAILS AND RESULTS

Experimental details can be found in the previous papers reporting results from the same measurement [38,39,41,43], and will not be repeated here. The multipolarity and electromagnetic character of the γ -ray transitions were determined on the basis of the directional correlation from oriented states ratios (R_{DCO}), two-point angular correlation (anisotropy) ratios (R_{ac}), and linear polarization (P), as described in Ref. [38].

The partial level scheme of ^{136}Nd showing the predicted zero- and one-phonon transverse wobbling bands L1 and L3 is plotted in Fig. 1. Band L3 was first identified in Ref. [34] and later confirmed in Refs. [36,39]. A clean γ -ray spectrum obtained by double gating on the 989- and 390-keV transitions is also shown in Fig. 1, in which the transitions have several thousands of counts, ensuring thus a sufficient precision for the measurement of the angular correlation and linear polarization.

Band L1 built on the 10^+ state has been reported and discussed previously in Refs. [34,36,37,39,42,43], and has spin-parity values firmly assigned up to spin 24^+ . The current work confirms all previous results. Band L3 consists of five levels with spin-parities from 13^+ to 21^+ , and decays to band L1 via the 768-, 785-, 751-, and 740-keV

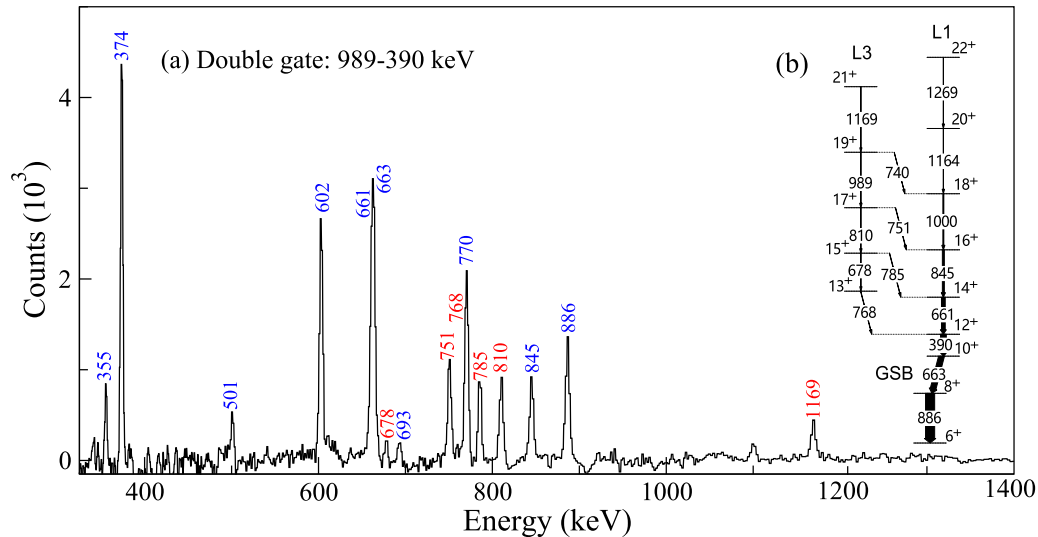


FIG. 1. (a) Double-gated spectrum on the 989- and 390-keV transitions showing the transitions in bands L1 and L3. The transitions of the ground state band and of band L1 are indicated in blue, while the transitions of band L3 are in red. The transitions in green are from other bands of ^{136}Nd [39] (355 keV between bands L1 and N1, 501 keV in band N1, and 693 keV between bands N1 and GSB). (b) Partial level scheme of ^{136}Nd relevant for the present work.

$\Delta I = 1$ transitions. For wobbling bands, these $\Delta I = 1$ transitions should have predominant $E2$ character [2–4,10]. Therefore, a high-precision measurement of the mixing ratio, $\delta(E2/M1)$, is crucial. In the present work, a combined linear polarization P and R_{ac} method was used to uniquely extract δ values of the connecting transitions between the one- and zero-phonon wobbling bands, as described in Refs. [46–50]. For such analysis, one should pay attention to use clean gates. Unfortunately, the 768-keV ($13^+ \rightarrow 12^+$) transition is strongly contaminated by the 770-keV transition of the ground state band (GSB), and therefore cannot be used to extract the linear polarization P , which is very sensitive to the number of counts. To analyze the 785-keV transition, one cannot use the 810-keV gate since a 811-keV transition is present in the γ band of ^{136}Nd , and therefore the 785-keV connecting transition will be contaminated by the 785-keV transition of band D5 and the 784-keV transition of band D6 located at higher spin in the level scheme of ^{136}Nd [39]. Another possible gate is on the 661-keV transition. However, such a gate will also induce the contamination from 784-keV transition of band D6 [39]. We therefore conclude that one cannot perform the polarization analysis of the 785-keV transition. The transition from band L3 to band L1 with the energy of 740 keV is too weak, no linear polarization value could be deduced. It should be also mentioned that another extraction method of mixing ratio is using the angular distribution alone, but this method always yield two solutions of mixing ratio, and one cannot safely exclude any of them only from the best fit of angular distribution curve, see Refs. [23–27].

The only connecting transition for which we could perform the combined P - R_{ac} analysis and extract its mixing ratio, is the 751-keV $17^+ \rightarrow 16^+$ transition. We selected the 989-keV gate to create the polarization spectra, since it leads to clean spectra, as demonstrated by the double-gated spectrum shown in Fig. 1, which only shows known transitions

of ^{136}Nd . The extracted R_{ac} ratio for the 751-keV transition is 0.55(5), indicating a mixed $M1$ and $E2$ character. The polarization asymmetry of $A_P = 0.03^{+0.06}_{-0.07}$ leads to a linear polarization of $P = 0.02^{+0.04}_{-0.05}$. Figure 2 provides the measured asymmetry spectra obtained by gating on 989 keV. One can distinguish the different behavior of the 770-keV, $4^+ \rightarrow 2^+$ transition of the GSB which has $E2$ character, from that of the 751-keV transition, ensuring thus the correctness of the present analysis. However, from these spectra, it is not easy to deduce the electromagnetic character of the transition, due to the very similar number of counts in the spectra

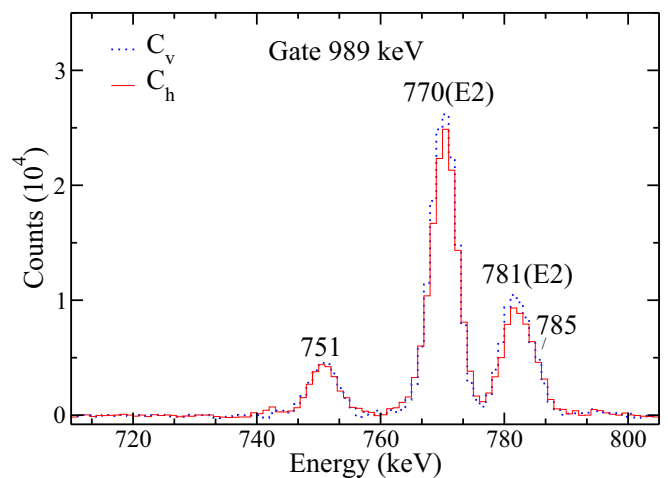


FIG. 2. Asymmetry spectra measured for the 751-keV ($17^+ \rightarrow 16^+$) transition in which the perpendicular (C_v) and parallel (C_h) spectra are marked with blue and red, respectively. The 781-keV γ ray is an intraband $E2$ transition in an other band of ^{136}Nd , which is in coincidence with the 989-keV, $15^- \rightarrow 13^-$ transition of band N1 in ^{136}Nd .

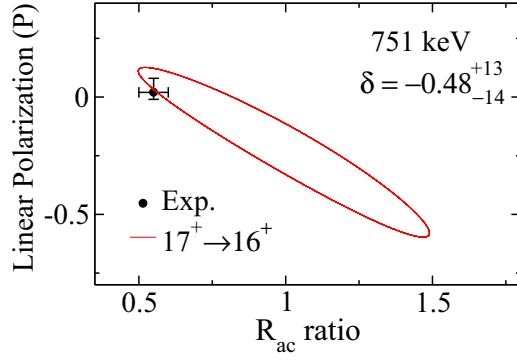


FIG. 3. Linear polarization (P) versus R_{ac} ratio for the 751-keV transition.

corresponding to perpendicular and parallel Compton scattering between the clover crystals. This is also the reason why we used the combination of polarization P and R_{ac} analyzes to extract the mixing ratios. The measured and calculated values of P and R_{ac} for the 751-keV transition are illustrated in Fig. 3. A mixing ratio of $\delta = -0.48_{-14}^{+13}$ is thus obtained. It corresponds to a 19% $E2$ component, a magnitude similar to the $E2$ component ($\approx 25\%$) for the transitions between the one- and zero-phonon wobbling bands $S1'$ and $S1$ in ^{130}Ba [32]. This amount of $E2$ component in the connecting transitions was attributed to the fact that two high- j quasiparticles are involved in the configuration of the bands $S1$ and $S1'$, which leads to larger $M1$ matrix elements than in the wobbling bands built on one-quasiparticle configurations and predominant magnetic character. The relative contribution of the $E2$ component to the $\Delta I = 1$ transitions is smaller than the $M1$ contribution, and therefore does not dominate like in the case of the one-quasiparticle bands of the odd-even wobblers [32]. The measured branching ratios $B(M1)_{\text{out}}/B(E2)_{\text{in}}$ and $B(E2)_{\text{out}}/B(E2)_{\text{in}}$ of the transitions depopulating the 17^+ state in ^{136}Nd are 0.61(29) and 0.36(17), respectively.

III. DISCUSSION

To investigate the nature of the motion leading to bands L1 and L3 in ^{136}Nd , we performed calculations with the semiclassical model coupling a triaxial core and a pair of quasiparticles rigidly aligned to the short axis introduced in Ref. [45] and based on Ref. [51]. The method prescribes a Schrödinger equation in a variable x associated with the total angular momentum projection on the medium axis:

$$\hat{H}_c = -\frac{1}{2} \frac{1}{\sqrt{B(x)}} \frac{d}{dx} \frac{1}{\sqrt{B(x)}} \frac{d}{dx} + V(x), \quad (1)$$

where

$$B(x) = \left[\frac{(2I-1)(I^2-x^2)(\mathcal{J}_l - \mathcal{J}_s)}{2\mathcal{J}_s\mathcal{J}_l} + \frac{j\sqrt{I^2-x^2}}{\mathcal{J}_s} \right]^{-1},$$

$$V(x) = \frac{I(\mathcal{J}_l + \mathcal{J}_s)}{4\mathcal{J}_l\mathcal{J}_s} + \frac{I^2}{2\mathcal{J}_m} + \frac{(2I-1)(I^2-x^2)(\mathcal{J}_m - \mathcal{J}_s)}{4I\mathcal{J}_m\mathcal{J}_s}$$

$$- \frac{j\sqrt{I^2-x^2}}{\mathcal{J}_s} + \frac{B''(x)}{8[B(x)]^2} - \frac{9[B'(x)]^2}{32[B(x)]^3}$$

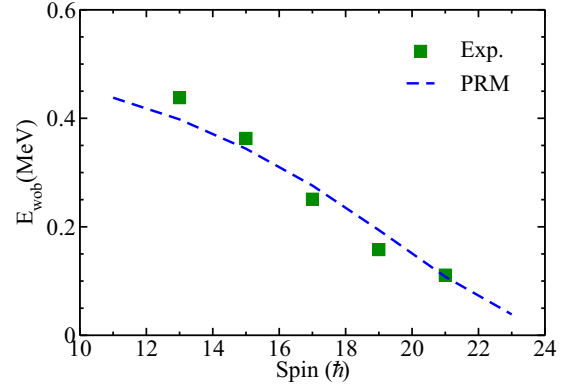


FIG. 4. Wobbling excitation energy versus spin for band L3. The errors on the experimental energies are smaller than the size of the symbols

are the coordinate-dependent effective mass and the wobbling potential, respectively, with $j = 10$ being the amount of spin alignment coming from the quasiparticle pair. The notation s, m, l stands for short, medium, and long semi-axes when hydrodynamic moments of inertia

$$\mathcal{J}_k = \frac{4}{3} \mathcal{J}_0 \sin^2 \left(\gamma - \frac{2}{3} k\pi \right), \quad k = 1, 2, 3 \quad (2)$$

are considered. The solutions of the constructed quantum Hamiltonian are confronted with the experimental energy levels and the associated electromagnetic properties, giving thus information on the deformation of the nucleus and specific evolution of the rotational dynamics with angular momentum. The theoretical energy to be compared with experimental data is expressed as

$$E(I, n) = E_{\text{diag}}[\mathcal{J}_0, \gamma; I(n+1)] + CI(I+1) + E_0, \quad (3)$$

where the energy obtained from the diagonalization of Eq. (1) is amended with a reference energy E_0 and a rotational correction which do not change the system's symmetry. The wobbling quantum number n is provided by the diagonalization solution's order and the associated eigenfunction is then used to define the coefficients of the total wave-function expansion in rotation matrices. The parameter values $\gamma = 23^\circ$, $\mathcal{J}_0 = 46.3$, $E_0 = 4.45$ MeV, and $C = 5.43$ keV [45] are determined by minimizing the sum of the rms values for the wobbling energy

$$E_{\text{wob}}(I) = E(I, 1) - \frac{1}{2}[E(I+1, 0) + E(I-1, 0)] \quad (4)$$

and the associated energy levels of the yrast band and the one-phonon wobbling band. The obtained triaxial deformation γ is consistent with that deduced, e.g., from the Coulomb excitation measurement of Ref. [52]. The consequent distribution of inertia about the long, short, and medium axes are 9.42, 22.3, 6 and 60.82 \hbar^2/MeV , respectively. The evolution with spin of the wobbling energy depends only on the triaxial deformation. As one can see in Fig. 4, the calculated wobbling excitation energy is in good agreement with experiment: it decreases with increasing spin, which is the characteristic behavior for a transverse coupling of the angular momenta of the unpaired nucleons and the core.

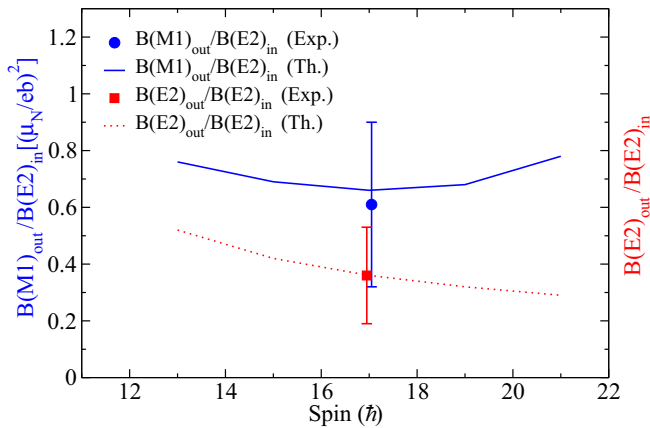


FIG. 5. Comparison between the experimental data (symbols) and calculated (lines) $B(M1)_{\text{out}}/B(E2)_{\text{in}}$ and $B(E2)_{\text{out}}/B(E2)_{\text{in}}$ ratios for the $\Delta I = 1$ transitions between bands L3 and L1 of ^{136}Nd .

For a realistic description of electric-quadrupole transition probabilities, it is necessary to include a second-order contribution to the $E2$ operator. As the γ deformation is already fixed from energy levels, its contribution relative to the usual first order $E2$ term is factorized by the product $(\chi\beta_2)$ [53], which is fixed by equating the theoretical formula with the single experimental $B(E2)_{\text{out}}/B(E2)_{\text{in}}$ data point. For example, considering the value $\beta_2 = 0.185$ tabulated in Ref. [54], the additional parameter then corresponds to $\chi = 2.14$. Figure 5 shows the extrapolation of the theoretical results from the experimental data point to other states, which are predicted to have a parabolic decrease with increasing spin. In what concerns the $B(M1)_{\text{out}}/B(E2)_{\text{in}}$ ratios, these are usually overestimated by an order of magnitude if one considers the usual quenching of the free spin gyromagnetic factor and the crude hydrodynamic estimation of Q entering in the quantity $(g_{\text{eff}}/Q)^2$ factorizing the ratio. Various quenching mechanisms [13,20,55] were adopted in order to match the experimental data and which can compensate the missing coupling of the wobbling and scissor-like excitations [56]. We chose to fix the quantity g_{eff}/Q by fitting the experimental $\Delta I = 1$ mixing ratio of the 751-keV transition. As one can see in Fig. 5, the predicted $B(M1)_{\text{out}}/B(E2)_{\text{in}}$ ratio is then well reproduced and has a higher curvature parabolic dependence on spin. Moreover, the model predicts an increase of $B(M1)_{\text{out}}/B(E2)_{\text{in}}$ values after $I = 17$, a behavior similar to that reported in Ref. [32] for the experimental data of the ^{130}Ba nucleus. However, the theoretical calculations made for ^{130}Ba [32] and the triaxial projected shell-model predictions [44] for the presently considered ^{136}Nd nucleus deliver instead a saturation of the $B(M1)_{\text{out}}/B(E2)_{\text{in}}$ ratio at higher spin states. This distinction can be attributed to the fact that

the high-spin experimental wobbling energy is overestimated by the calculations of Ref. [44] due to the depleting of the quasiparticle alignment on the short axis which is otherwise kept *a priori* rigid in the present model.

We note that calculations similar to those for ^{130}Ba [32] employing the constrained triaxial covariant density functional theory combined with the quantum particle rotor model [57] also leads to a good agreement with the experimental results for bands L1 and L3 of ^{136}Nd , revealing the presence of transverse wobbling type of motion in the assigned two-quasiparticle $\pi h_{11/2}^2$ configurations.

IV. SUMMARY

In summary, the present paper reports the necessary experimental evidence of the transverse wobbling nature of two medium-spin bands in ^{136}Nd , predicted by triaxial projected shell-model calculations. The experimental mixing ratio for one $\Delta I = 1$ transition linking bands L1 and L3 in ^{136}Nd based on the two-quasiparticle $\pi h_{11/2}^2$ configuration has been determined based on combined R_{ac} and polarization measurements. The wobbling excitation energies and the ratios of reduced transition probabilities calculated using a new particle rotor model which rigidly couples the total angular momentum of two quasiparticles to that of a triaxial core in an orthogonal geometry are in good agreement with experimental data, supporting the interpretation of the bands as the second example of transverse wobbling bands in even-even nuclei.

ACKNOWLEDGMENTS

This work has been supported by the Special Research Assistant Project of the Chinese Academy of Sciences; by the Strategic Priority Research Program of Chinese Academy of Sciences (Grant No. XDB34000000); by the Academy of Finland under the Finnish Centre of Excellence Programme (2012-2017); by the EU 7th Framework Programme Project No. 262010 (ENSAR); by the French Ministry of Foreign Affairs and the Ministry of Higher Education and Research, France (PHC PROTEA Grant No. 42417SE); by the National Research, Development and Innovation Fund of Hungary (Project No. K128947), as well as by the European Regional Development Fund (Contract No. GINOP-2.3.3-15-2016-00034); by the Polish National Science Centre (NCN) Grant No. 2013/10/M/ST2/00427; by the Swedish Research Council under Grant No. 621-2014-5558. The use of germanium detectors from the GAMMAPOOL is acknowledged. I.K. was supported by National Research, Development and Innovation Office-NKFIH, Contract No. PD 124717. R.B. acknowledges the financial support of the Romanian Ministry of Research, Innovation and Digitalization, through Project No. PN-19-06-01-01/2019-2022.

- [1] A. Bohr and B. R. Mottelson, *Nuclear Structure* (Benjamin, New York, 1975), Vol. I.
- [2] P. Bringel *et al.*, *Eur. Phys. J. A* **24**, 167 (2005).
- [3] S. W. Odegård, G. B. Hagemann, D. R. Jensen, M. Bergstrom, B. Herskind, G. Sletten, S. Tormanen, J. N. Wilson, P. O. Tjorn,

- I. Hamamoto, K. Spohr, H. Hubel, A. Gorgen, G. Schonwasser, A. Bracco, S. Leoni, A. Maj, C. M. Petrache, P. Bednarczyk, and D. Curien, *Phys. Rev. Lett.* **86**, 5866 (2001).
- [4] D. R. Jensen, G. B. Hagemann, I. Hamamoto, S. W. Odegard, B. Herskind, G. Sletten, J. N. Wilson, K. Spohr, H. Hubel,

- P. Bringel, A. Neusser, G. Schonwasser, A. K. Singh, W. C. Ma, H. Amro, A. Bracco, S. Leoni, G. Benzoni, A. Maj, C. M. Petrache, G. Lo Bianco, P. Bednarczyk, and D. Curien, *Phys. Rev. Lett.* **89**, 142503 (2002).
- [5] G. Schönwaßer *et al.*, *Phys. Lett. B* **552**, 9 (2003).
- [6] H. Amro *et al.*, *Phys. Lett. B* **553**, 197 (2003).
- [7] D. J. Hartley, R. V. F. Janssens, L. L. Riedinger, M. A. Riley, A. Aguilar, M. P. Carpenter, C. J. Chiara, P. Chowdhury, I. G. Darby, U. Garg, Q. A. Ijaz, F. G. Kondev, S. Lakshmi, T. Lauritsen, A. Ludington, W. C. Ma, E. A. McCutchan, S. Mukhopadhyay, R. Pifer, E. P. Seyfried, I. Stefanescu, S. K. Tandel, U. Tandel, J. R. Vanhoy, X. Wang, S. Zhu, I. Hamamoto, and S. Frauendorf, *Phys. Rev. C* **80**, 041304(R) (2009).
- [8] I. Hamamoto, *Phys. Rev. C* **65**, 044305 (2002).
- [9] I. Hamamoto and G. B. Hagemann, *Phys. Rev. C* **67**, 014319 (2003).
- [10] S. Frauendorf and F. Döna, *Phys. Rev. C* **89**, 014322 (2014).
- [11] J. T. Matta, U. Garg, W. Li, S. Frauendorf, A. D. Ayangeakaa, D. Patel, K. W. Schllax, R. Palit, S. Saha, J. Sethi, T. Trivedi, S. S. Ghugre, R. Raut, A. K. Sinha, R. V. F. Janssens, S. Zhu, M. P. Carpenter, T. Lauritsen, D. Seweryniak, C. J. Chiara, F. G. Kondev, D. J. Hartley, C. M. Petrache, S. Mukhopadhyay, D. V. Lakshmi, M. K. Raju, P. V. MadhusudhanaRao, S. K. Tandel, S. Ray, and F. Döna, *Phys. Rev. Lett.* **114**, 082501 (2015).
- [12] N. Sensharma *et al.*, *Phys. Lett. B* **792**, 170 (2019).
- [13] J. Timar, Q. B. Chen, B. Kruzsicz, D. Sohler, I. Kuti, S. Q. Zhang, J. Meng, P. Joshi, R. Wadsworth, K. Starosta, A. Algora, P. Bednarczyk, D. Curien, Z. Dombradi, G. Duchene, A. Gizon, J. Gizon, D. G. Jenkins, T. Koike, A. Krasznahorkay, J. Molnar, B. M. Nyako, E. S. Paul, G. Rainovski, J. N. Scheurer, A. J. Simons, C. Vaman, and L. Zolnai, *Phys. Rev. Lett.* **122**, 062501 (2019).
- [14] S. Biswas *et al.*, *Eur. Phys. J. A* **55**, 159 (2019).
- [15] N. Sensharma, U. Garg, Q. B. Chen, S. Frauendorf, D. P. Burdette, J. L. Cozzi, K. B. Howard, S. Zhu, M. P. Carpenter, P. Copp, F. G. Kondev, T. Lauritsen, J. Li, D. Seweryniak, J. Wu, A. D. Ayangeakaa, D. J. Hartley, R. V. F. Janssens, A. M. Forney, W. B. Walters, S. S. Ghugre, and R. Palit, *Phys. Rev. Lett.* **124**, 052501 (2020).
- [16] S. Nandi, G. Mukherjee, Q. B. Chen, S. Frauendorf, R. Banik, S. Bhattacharya, S. Dar, S. Bhattacharyya, C. Bhattacharya, S. Chatterjee, S. Das, S. Samanta, R. Raut, S. S. Ghugre, S. Rajbanshi, S. Ali, H. Pai, M. A. Asgar, S. Das Gupta, P. Chowdhury, and A. Goswami, *Phys. Rev. Lett.* **125**, 132501 (2020).
- [17] S. Chakraborty *et al.*, *Phys. Lett. B* **811**, 135854 (2020).
- [18] E. A. Lawrie, O. Shirinda, and C. M. Petrache, *Phys. Rev. C* **101**, 034306 (2020).
- [19] B. F. Lv, C. M. Petrache, E. A. Lawrie, A. Astier, E. Dupont, K. K. Zheng, P. Greenlees, H. Badran, T. Calverley, D. M. Cox, T. Grahn, J. Hilton, R. Julin, S. Juutinen, J. Konki, J. Pakarinen, P. Papadakis, J. Partanen, P. Rakhila, P. Ruotsalainen, M. Sandzelius, J. Saren, C. Scholey, J. Sorri, S. Stolze, J. Uusitalo, B. Cederwall, A. Ertoprak, H. Liu, S. Guo, J. G. Wang, H. J. Ong, X. H. Zhou, Z. Y. Sun, I. Kuti, J. Timar, A. Tucholski, J. Srebrny, and C. Andreoiu, *Phys. Rev. C* **103**, 044308 (2021).
- [20] A. A. Raduta, R. Poenaru, and C. M. Raduta, *Phys. Rev. C* **101**, 014302 (2020).
- [21] K. Tanabe and K. Sugawara-Tanabe, *Phys. Rev. C* **95**, 064315 (2017).
- [22] K. Tanabe and K. Sugawara-Tanabe, *Phys. Rev. C* **97**, 069802 (2018).
- [23] B. F. Lv *et al.*, *Phys. Lett. B* **824**, 136840 (2022).
- [24] S. Guo *et al.*, submitted to *Phys. Lett. B*, arXiv:2011.14354.
- [25] S. Guo, arXiv:2011.14364.
- [26] S. Guo and C. M. Petrache, arXiv:2007.10031v2.
- [27] R. Garg, S. Kumar, M. Saxena, S. Goyal, D. Siwal, S. Kalkal, S. Verma, R. Singh, S. C. Pancholi, R. Palit, D. Choudhury, S. S. Ghugre, G. Mukherjee, R. Kumar, R. P. Singh, S. Muralithar, R. K. Bhowmik, and S. Mandal, *Phys. Rev. C* **100**, 069901(E) (2019).
- [28] K. Nomura and C. M. Petrache, *Phys. Rev. C* **105**, 024320 (2022).
- [29] J. H. Hamilton *et al.*, *Nucl. Phys. A* **834**, 28c (2010).
- [30] Y. X. Luo *et al.*, in *Exotic Nuclei: Exon-2012: Proceedings of the International Symposium* (World Scientific, Singapore, 2013).
- [31] C. M. Petrache and S. Guo, arXiv:1603.08247.
- [32] Q. B. Chen, S. Frauendorf, and C. M. Petrache, *Phys. Rev. C* **100**, 061301(R) (2019).
- [33] E. Mergel *et al.*, *Eur. Phys. J. A* **15**, 417 (2002).
- [34] E. S. Paul, C. W. Beausang, D. B. Fossan, R. Ma, W. F. Piel, Jr., P. K. Weng, and N. Xu, *Phys. Rev. C* **36**, 153 (1987).
- [35] S. Mukhopadhyay, D. Almeded, U. Garg, S. Frauendorf, T. Li, P. V. Madhusudhana Rao, X. Wang, S. S. Ghugre, M. P. Carpenter, S. Gros, A. Hecht, R. V. F. Janssens, F. G. Kondev, T. Lauritsen, D. Seweryniak, and S. Zhu, *Phys. Rev. C* **78**, 034311 (2008).
- [36] C. M. Petrache *et al.*, *Phys. Lett. B* **373**, 275 (1996).
- [37] S. Perries, A. Astier, L. Ducroux, M. Meyer, N. Redon, C. M. Petrache, D. Bazzacco, G. Falconi, S. Lunardi, M. Lunardon, C. RossiAlvarez, C. A. Ur, R. Venturelli, G. Viesti, I. Deloncle, M. G. Porquet, G. de Angelis, M. de Poli, C. Fahlander, E. Farnea, D. Foltescu, A. Gadea, D. R. Napoli, Z. Podolyak, A. Bracco, S. Frattini, S. Leoni, B. Cederwall, A. Johnson, and R. A. Wyss, *Phys. Rev. C* **60**, 064313 (1999).
- [38] C. M. Petrache, B. F. Lv, A. Astier, E. Dupont, Y. K. Wang, S. Q. Zhang, P. W. Zhao, Z. X. Ren, J. Meng, P. T. Greenlees, H. Badran, D. M. Cox, T. Grahn, R. Julin, S. Juutinen, J. Konki, J. Pakarinen, P. Papadakis, J. Partanen, P. Rakhila, M. Sandzelius, J. Saren, C. Scholey, J. Sorri, S. Stolze, J. Uusitalo, B. Cederwall, O. Aktas, A. Ertoprak, H. Liu, S. Matta, P. Subramaniam, S. Guo, M. L. Liu, X. H. Zhou, K. L. Wang, I. Kuti, J. Timar, A. Tucholski, J. Srebrny, and C. Andreoiu, *Phys. Rev. C* **97**, 041304(R) (2018).
- [39] B. F. Lv, C. M. Petrache, A. Astier, E. Dupont, A. Lopez-Martens, P. T. Greenlees, H. Badran, T. Calverley, D. M. Cox, T. Grahn, J. Hilton, R. Julin, S. Juutinen, J. Konki, M. Leino, J. Pakarinen, P. Papadakis, J. Partanen, P. Rakhila, M. Sandzelius, J. Saren, C. Scholey, J. Sorri, S. Stolze, J. Uusitalo, A. Herzan, B. Cederwall, A. Ertoprak, H. Liu, S. Guo, M. L. Liu, Y. H. Qiang, J. G. Wang, X. H. Zhou, I. Kuti, J. Timar, A. Tucholski, J. Srebrny, and C. Andreoiu, *Phys. Rev. C* **98**, 044304 (2018).
- [40] Q. B. Chen, B. F. Lv, C. M. Petrache, and J. Meng, *Phys. Lett. B* **782**, 744 (2018).
- [41] C. M. Petrache, N. Minkov, T. Nakatsukasa, B. F. Lv, A. Astier, E. Dupont, K. K. Zheng, P. Greenlees, H. Badran, T. Calverley, D. M. Cox, T. Grahn, J. Hilton, R. Julin, S. Juutinen, J. Konki, J. Pakarinen, P. Papadakis, J. Partanen, P. Rakhila, P. Ruotsalainen, M. Sandzelius, J. Saren, C. Scholey, J. Sorri, S. Stolze, J. Uusitalo, B. Cederwall, A. Ertoprak, H. Liu, S.

- Guo, M. L. Liu, J. G. Wang, X. H. Zhou, I. Kuti, J. Timar, A. Tucholski, J. Srebrny, and C. Andreoiu, *Phys. Rev. C* **102**, 014311 (2020).
- [42] A. Tucholski, C. Droste, J. Srebrny, C. M. Petrache, J. Skalski, P. Jachimowicz, M. Fila, T. Abraham, M. Kisielinski, A. Kordyasz, M. Kowalczyk, J. Kownacki, T. Marchlewski, P. J. Napiorkowski, L. Prochniak, J. Samorajczyk-Pysk, A. Stolarz, A. Astier, B. F. Lv, E. Dupont, S. Lalkovski, P. Walker, E. Grodner, and Z. Patyk, *Phys. Rev. C* **100**, 014330 (2019).
- [43] C. M. Petrache, B. F. Lv, A. Astier, E. Dupont, K. K. Zheng, P. T. Greenlees, H. Badran, T. Calverley, D. M. Cox, T. Grahn, J. Hilton, R. Julin, S. Juutinen, J. Konki, J. Pakarinen, P. Papadakis, J. Partanen, P. Rahkila, P. Ruotsalainen, M. Sandzelius, J. Saren, C. Scholey, J. Sorri, S. Stolze, J. Uusitalo, B. Cederwall, O. Aktas, A. Ertoprak, H. Liu, S. Guo, M. L. Liu, J. G. Wang, X. H. Zhou, I. Kuti, J. Timar, A. Tucholski, J. Srebrny, and C. Andreoiu, *Phys. Rev. C* **100**, 054319 (2019).
- [44] F.-Q. Chen and C. M. Petrache, *Phys. Rev. C* **103**, 064319 (2021).
- [45] R. Budaca and C. M. Petrache (unpublished).
- [46] A. Krämer-Flecken, T. Morek, R. M. Lieder, W. Gast, G. Hebbinghaus, H. M. Jäger, and W. Urban, *Nucl. Instrum. Methods Phys. Res., Sect. A* **275**, 333 (1989).
- [47] C. J. Chiara, M. Devlin, E. Ideguchi, D. R. LaFosse, F. Lerma, W. Reviol, S. K. Ryu, D. G. Sarantites, O. L. Pechenaya, C. Baktash, A. Galindo-Uribarri, M. P. Carpenter, R. V. F. Janssens, T. Lauritsen, C. J. Lister, P. Reiter, D. Seweryniak, P. Fallon, A. Gorgen, A. O. Macchiavelli, D. Rudolph, G. Stoitcheva, and W. E. Ormand, *Phys. Rev. C* **75**, 054305 (2007).
- [48] C. Droste *et al.*, *Nucl. Instrum. Methods Phys. Res., Sect. A* **378**, 518 (1996).
- [49] K. Starosta *et al.*, *Nucl. Instrum. Methods Phys. Res., Sect. A* **423**, 16 (1999).
- [50] A. Herzáň, S. Juutinen, K. Auranen, T. Grahn, P. T. Greenlees, K. Hauschild, U. Jakobsson, P. Jones, R. Julin, S. Ketelhut, M. Leino, A. Lopez-Martens, P. Nieminen, M. Nyman, P. Peura, P. Rahkila, S. Rinta-Antila, P. Ruotsalainen, M. Sandzelius, J. Saren, C. Scholey, J. Sorri, and J. Uusitalo, *Phys. Rev. C* **92**, 044310 (2015).
- [51] R. Budaca, *Phys. Lett. B* **797**, 134853 (2019).
- [52] T. R. Saito *et al.*, *Phys. Lett. B* **669**, 19 (2008).
- [53] M. A. Caprio and F. Iachello, *Nucl. Phys. A* **781**, 26 (2007).
- [54] P. Möller, A. J. Sierk, T. Ichikawa, and H. Sagawa, *At. Data Nucl. Data Tables* **109-110**, 1 (2016).
- [55] R. Budaca, *Phys. Rev. C* **103**, 044312 (2021).
- [56] S. Frauendorf and F. Döna, *Phys. Rev. C* **92**, 064306 (2015).
- [57] Q. B. Chen (private communication).